EQUIPARTITIONING IN A HIGH CURRENT PROTON LINAC*

Lloyd M. Young

Los Alamos National Laboratory, MS H817, Los Alamos, NM 87545, USA

Abstract

The code PARMILA simulates the beam transmission through the Accelerator for the Production of Tritium (APT) linac. The beam is equipartitioned when the longitudinal and transverse temperatures are equal. This paper explores the consequence of equipartitioning in the APT linac. The simulations begin with a beam that starts at the ion-source plasma surface. PARMILA tracks the particles from the RFQ exit through the 1.7-GeV linac. This paper compares two focusing schemes. One scheme uses mostly equal strength quadrupoles. The equipartitioning scheme uses weaker focusing in the high-energy portion of the linac. The RMS beam size with the equipartitioning scheme is larger, but the relative size of the halo is less than in the equal-strength design.

INTRODUCTION

R. Jameson and Martin Reiser recommend tailoring the transverse focusing in high-current linacs to equipartition [1,2] the beam. To explore the merits of equipartitioning I compare simulations of the beam distributions through two linacs, one with equipartitioning and one without equipartitioning. The two linacs are identical up to 25 MeV. In both cases the simulations follow the same particle collection to the end of the linac at 1.7 GeV. The code PARMELA [3] simulates the transport of the beam through the ion source extractor and the low-energy beam-transport line (LEBT) to the radio frequency quadrupole (RFQ) [4]. PARMELA uses electrons to simulate space charge neutralization in the first 40 cm of the LEBT. For the remainder of the LEBT, PARMELA simulates space charge neutralization by reducing the effective charge to 4% of the proton-beam charge. The input distribution to the RFQ obtained this way is quite different from the "type 6" distribution normally used in the code PARMTEQM [5]. This beam is rotating in real space because it is "born" in the longitudinal magnetic field of the ion source. It also has a hole in the center. The code PARMTEQM generates the "type 6" distribution by placing the particles randomly in a four-dimensional transverse hyperspace with uniform phase and no energy spread. The beam current after the RFQ was 100 mA. PARMELA, PARMTEQM, and PARMILA[6] performed all of the simulations shown in this paper with 100,000 macro particles.

THE EQUIPARTITIONING CONCEPT

Equipartitioning implies: $\varepsilon_x^2/x_{rms}^2 = \varepsilon_y^2/y_{rms}^2 = \varepsilon_z^2/(\gamma \cdot z_{rms})^2$, where γ is the relativistic ratio of total energy to rest mass, ε_x, ε_y, and ε_z are the normalized emittances for the transverse and longitudinal coordinates respectively. The

respective RMS beam sizes are x_{rms}, y_{rms}, and z_{rms}. The RFQ, the coupled-cavity drift-tube linac (CCDTL), the coupled-cavity linac (CCL), and the superconducting (SC) linac have alternating gradient quadrupole focusing channels. These focusing channels cause the x_{rms} and y_{rms} values to oscillate about the equilibrium value $\sim \sqrt{x_{rms} \cdot y_{rms}}$. Therefore, averaging over these oscillations the partitioning ratios *Ax* and *Ay* are defined as:

$$Ax = \gamma^2 \left(\frac{\varepsilon_x^2}{x_{rms} \cdot y_{rms}} \right) \cdot \left(\frac{z_{rms}^2}{\varepsilon_z^2} \right), \quad Ay = \gamma^2 \left(\frac{\varepsilon_y^2}{x_{rms} \cdot y_{rms}} \right) \cdot \left(\frac{z_{rms}^2}{\varepsilon_z^2} \right).$$

Because the transverse emittances ε_x and ε_y are nearly equal, Ax and Ay will fall on top of each other when plotted.

THE RADIAL DISTRIBUTION

Comparison of Figures 1 and 2 shows that the particle distribution at the exit of the linac has no halo from the equipartitioned linac and a large halo from the nonequipartitioned linac.
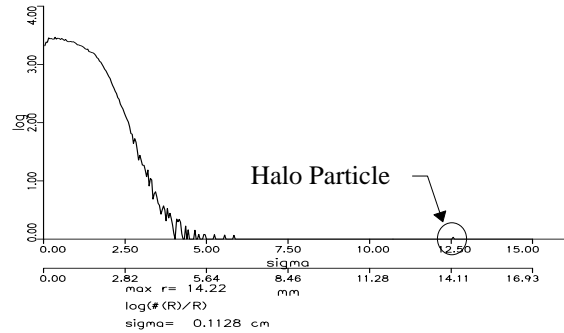

Figure 1. The logarithm of particle density versus radius in the nonequipartitioned linac.
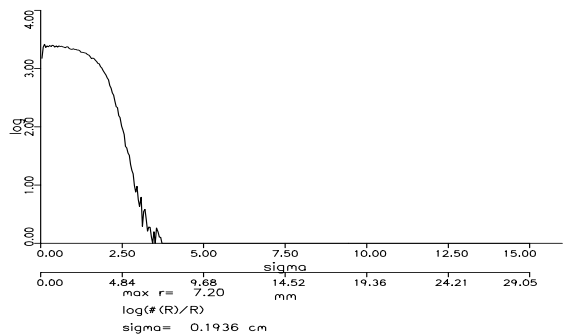

Figure 2. The distribution at the end of the equipartitioned linac.

These figures show the transverse distributions and the extent of the tail. The plots of the radial distribution are generated by populating the elements of an array

---

according to each particles' radial position **r**. The beam distribution is first normalized to circular symmetry. For example, if x_{rms} is smaller than y_{rms} all the x coordinates are multiplied by y_{rms}/x_{rms} then $r = \sqrt{y^2 + (x \cdot y_{rms}/x_{rms})^2}$. To plot the logarithm of this array we initialize the array elements to 1. Each element, which corresponds to a small range of r values, is increased by 1/r for each particle so that the final array gives the distribution of local particle density. The plots show the radial density distribution versus distance from the center of the beam. The upper abscissa on these plot has units of σ, the standard deviation, where σ is the larger of x_{rms} and y_{rms}. The lower abscissa is in mm.

The distribution in Figure 1 extends beyond 12 σ, while the largest particle radius occurs at 14.2 mm. In Figure 2 (the equipartitioned case) the distribution extends only to ~4 σ, and the largest radius is 7.2 mm. The beam expander and target designers prefer the distribution from the equipartitioned linac because the tails of the beam do not extend as far.

Figure 3 shows the zero-current phase advance in the nonequipartitioned linac from 100 keV to 1.7 GeV. Note that σ_{0l}/σ_{0t}, the ratio of the longitudinal phase advance to the transverse phase advance, increases beyond 25 MeV. Figure 4 shows the zero-current phase advance in the equipartitioned linac, where σ_{0l}/σ_{0t} is nearly constant throughout the linac. **Equipartitioning requires only this slight difference in the transverse focusing strength above 25 MeV.** The quadrupole strength at the end of the equipartitioned linac is 55% of the strength in the nonequipartitioned linac.
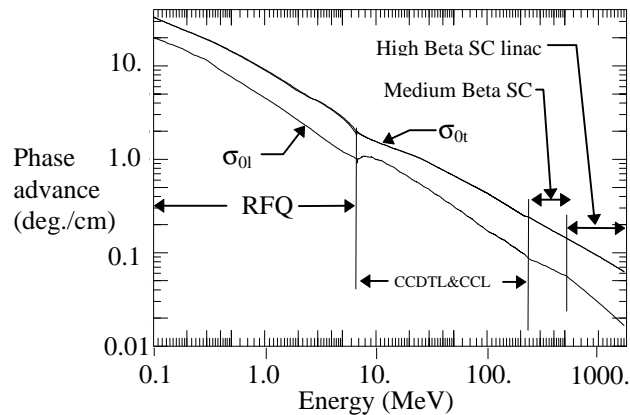

Figure 3. The zero-current phase advance σ_x, σ_y, and σ_l per unit length in the nonequipartitioned linac.

The APT linac uses normal conducting (NC) structures up to 217 MeV, and SC cavities from 217 MeV to 1.7 GeV. The NC linac consists of a 6.7-MeV RFQ, a CCDTL to 100 MeV, and a CCL to 217 MeV. PARMILA calculates the phase advance in the SC linac by averaging over one period of the lattice consisting of accelerating cavities and quadrupole magnets. The period in the SC linac is much longer than in the NC linac where the period spans two quadrupoles. A cryomodule has three SC cavities in the medium-β section (217 MeV to 469 MeV) and four SC cavities in the high-β section (469 MeV to the end). If the

space between cryomodules contained an accelerating cavity the two-quadrupole period of the magnetic lattice would have been preserved. However, this warm space between the cryomodules is used by the valves and beam diagnostics. Therefore, the period in the medium-β section now spans four quadrupoles instead of two. In the high-β SC linac the period spans 10 quadrupoles.
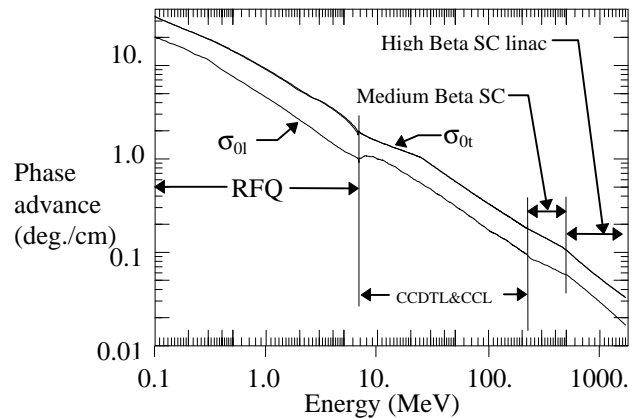

Figure 4. The zero-current phase advance σ_x, σ_y, and σ_l per unit length in the equipartitioned linac.

Figures 5 and 6 show the partitioning ratios Ax and Ay through the RFQ to the end of the linac. The slight excess of the longitudinal focusing between 7 and 20 MeV does not appear to cause any problems. The transverse focusing is as strong as the 8 βλ period allows in this region. The only way to correct the equipartitioning ratio in this region is the use of a more gradual increase in the accelerating gradient.
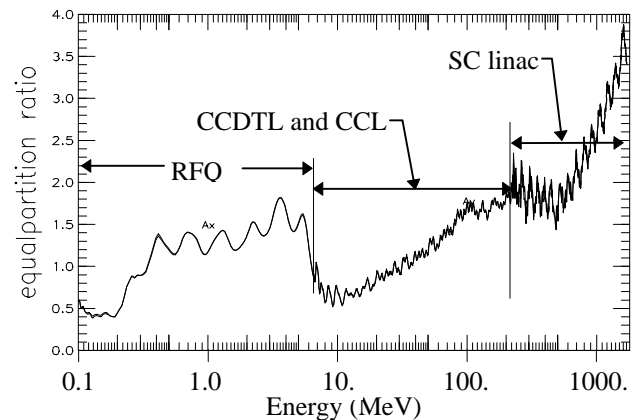

Figure 5. The partitioning ratio Ax and Ay in the nonequipartitioned linac.

Although it is desirable to have these ratios near unity, they are extremely sensitive to mismatch. A slight mismatch at the entrance to the RFQ and CCDTL causes the oscillations of *Ax* and *Ay* in these figures. A larger mismatch between the CCL and the SC linac causes the large oscillations starting at 217 MeV.

The partitioning ratios are greater than 1.0 in most of the RFQ. In this structure we deliberately use strong transverse focusing relative to the longitudinal focusing to minimize the beam loss. Any halo that develops in the RFQ is scraped off on the RFQ vanes. The smaller longitudinal acceptance of the 700-MHz CCDTL

compared to the 350-MHz RFQ required relatively stronger longitudinal focusing. This bias toward reducing beam loss in designing the APT front end resulted in partitioning ratios greater than 1 in the RFQ and less then 1 near the end of the RFQ and in the low-energy portion of the CCDTL. For higher beam energy, the longitudinal focusing weakens faster than the transverse focusing does. Thus, for fixed accelerating gradient, the partitioning ratios tend to grow at high energy without a reduction in the transverse focusing. (The accelerating gradient is limited by power loss considerations in the NC linac and by peak electric field in the SC linac.)
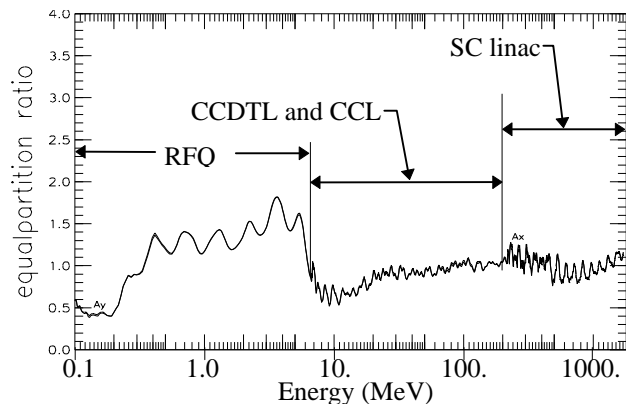

Figure 6. The partitioning ratio Ax and Ay in the equipartitioned linac.

In the equipartitioned linac the quadrupole strength tapers off slowly with increasing energy from the 25-MeV point to the end of the linac. Figure 6 shows the ratios Ax and Ay in the equipartitioned linac. To match the transverse focusing in the CCL to the SC linac, the quadrupole strength in the nonequipartitioned linac is also reduced with increasing energy from 100 MeV to 217 MeV. This reduction smoothly matches the transverse focusing in the CCL to the transverse focusing in the SC linac, which has a longer period.

From 217 MeV to 469 MeV, in both the equipartitioned linac and the nonequipartitioned linac the synchronous phase slowly increases from $-25°$ to $-35°$, while the strength of the quadrupoles remains constant. This phase ramp matches the longitudinal focusing of the CCL to the medium-β SC section and the medium-β to the high-β SC section. The high-β SC section has a higher average accelerating gradient than the medium-β SC section. The CCL and the high-β SC section both have a synchronous phase of $-30°$. Coincidentally in the equipartitioned linac, this phase ramp tailors the longitudinal focusing sufficiently to maintain the partitioning ratio close to 1.

Comparison of the beam size shown in Figs. 7 and 8 for the two designs shows that a halo develops in the nonequipartitioned linac, but not in the equipartitioned linac. This halo extends to about 12 times the RMS beam size. In the beam-dynamics simulations the halo develops in the NC accelerator between 50 and 100 MeV. In both simulations, the beam is matched in exactly the same.
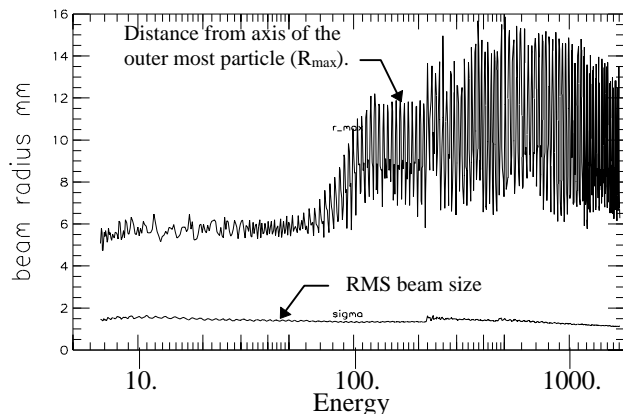

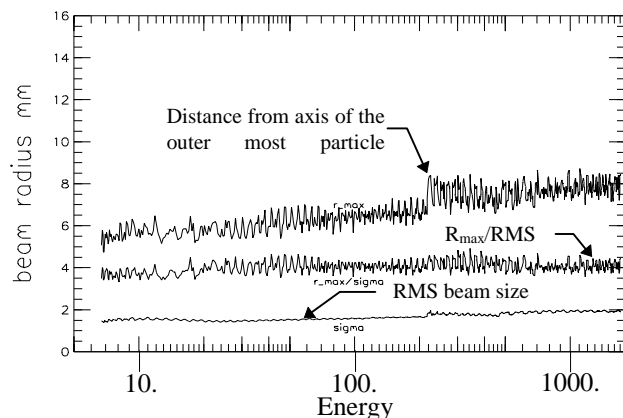Figure 7. Beam size in the nonequipartitioned linac.

Figure 8. Beam size in the equipartitioned linac. The ratio R_{max}/(RMS beam size) is also plotted.

CONCLUSIONS

Virtually no halo developed in the equipartitioned linac with some mismatch while a substantial halo developed in the nonequipartitioned linac. Other simulations, not presented here, show that a large mismatch will cause halo to develop in an equipartitioned linac, but to less extent relative to the rms beam size than in a nonequipartitioned linac.

REFERENCES

[1] R. A. Jameson, "On Scaling & Optimization of High Intensity, Low-Beam-Loss RF Linacs for Neutron Source Drivers", AIP Conf. Proc. 279, ISBN 1-56396-191-1, DOE Conf-9206193 (1992) 969-998, Proc. Third Workshop on Advanced Accelerator Concepts, 14-20 June 1992, Port Jefferson, Long Island, NY, (LA-UR-92-2474, Los Alamos National Laboratory).

[2] Martin Reiser, "Theory and Design of Charged Particle Beams," John Wiley & Sons, Inc., p. 573 (1994).

[3] L. M. Young and J. H. Billen, "PARMELA," Los Alamos National Laboratory report LA-UR-96-1835 (revision March 14, 1997).

[4] L. M. Young, "Simulations of the LEDA RFQ 6.7 MeV Accelerator", this conference.

[5] Kenneth R. Crandall, et al., "RFQ Design Codes," Los Alamos National Laboratory report LA-UR-96-1836 (revision February 12, 1997).

[6] H. Takeda and J. E. Stovall, "Modified PARMILA Code for New Accelerating Structures," Proc. of the 1995 Particle Accelerator Conf, p. 2364 (May 1-5, 1995, Dallas, Texas).